

# Investigation of compression ratio and fuel effect on combustion and PM emissions in a DISI engine

Lattimore, T. , Herreros, J. M. , Xu, H. and Shuai, S.

**Author post-print (accepted) deposited by Coventry University's Repository**

**Original citation & hyperlink:**

Lattimore, T. , Herreros, J. M. , Xu, H. and Shuai, S. (2016) Investigation of compression ratio and fuel effect on combustion and PM emissions in a DISI engine. Fuel, volume 169 : 68-78  
<http://dx.doi.org/10.1016/j.fuel.2015.10.044>

DOI 10.1016/j.fuel.2015.10.044

ISSN 0016-2361

ESSN 1873-7153

Publisher: Elsevier

**NOTICE: this is the author's version of a work that was accepted for publication in Fuel. Changes resulting from the publishing process, such as peer review, editing, corrections, structural formatting, and other quality control mechanisms may not be reflected in this document. Changes may have been made to this work since it was submitted for publication. A definitive version was subsequently published in Fuel, [VOL 169, (2015)] DOI: 10.1016/j.fuel.2015.10.044**

© 2015, Elsevier. Licensed under the Creative Commons Attribution-NonCommercial-NoDerivatives 4.0 International

<http://creativecommons.org/licenses/by-nc-nd/4.0/>

Copyright © and Moral Rights are retained by the author(s) and/ or other copyright owners. A copy can be downloaded for personal non-commercial research or study, without prior permission or charge. This item cannot be reproduced or quoted extensively from without first obtaining permission in writing from the copyright holder(s). The content must not be changed in any way or sold commercially in any format or medium without the formal permission of the copyright holders.

This document is the author's post-print version, incorporating any revisions agreed during the peer-review process. Some differences between the published version and this version may remain and you are advised to consult the published version if you wish to cite from it.

# Investigation of Compression Ratio and Fuel Effect on Combustion and PM Emissions in a DISI Engine

Thomas Lattimore<sup>1</sup>, Jose Martin Herreros<sup>1</sup>, Hongming Xu<sup>1,2\*</sup>, Shijin Shuai<sup>2</sup>

1. University of Birmingham, Birmingham, B15 2TT, UK

2. State Key Laboratory of Automotive Safety and Energy, Tsinghua University, Beijing

## Abstract

Oxygenated fuel components such as the alcohols of 1-butanol and ethanol are well-known for their potential to improve engine combustion and PM emissions, and these particular fuels are receiving ever greater attention due to their renewable nature giving them great CO<sub>2</sub> emission reduction potential. This paper investigates the effect of compression ratio and fuel properties on combustion, gaseous emissions and PM emissions of an experimental single-cylinder direct injection spark ignition (DISI) engine. The tests were carried out at an engine load of 8.5 bar, at various compression ratios between 10.7 and 11.5, with Bu20 (20% vol 1-butanol in gasoline) and E20 (20% vol ethanol in gasoline) fuel blends along with a reference fuel of gasoline. The results show that 1-butanol and ethanol addition to gasoline is effective to advance the MFB50 point and shorten the combustion duration. 1-butanol addition to gasoline is effective to reduce PM number emissions, while NO<sub>x</sub> reduction is the main benefit of ethanol addition. It is concluded that synergies between compression ratio and alcohol addition to gasoline enable to simultaneously control gaseous and particulate matter emissions while improving fuel economy with respect to standard gasoline combustion.

**Keywords:** Compression Ratio; Butanol; DISI; Emissions; Particulates

\* Corresponding author. Tel.: +44 121 4144153; fax: +44 121 4143958.

E-mail address: h.m.xu@bham.ac.uk (Hongming Xu).

## 27 **1.0 Introduction**

28  
29 Reducing net CO<sub>2</sub> emissions from the transportation sector is at the forefront of public  
30 perception due to environmental protection concerns. One way to reduce engine CO<sub>2</sub> output  
31 is to increase engine's compression ratio; this improves its thermal efficiency causing the fuel  
32 consumption and thus CO<sub>2</sub> emissions to reduce. Another way to reduce net CO<sub>2</sub> output is to  
33 convert biomass to produce renewable oxygenated fuels to be used in the transportation and  
34 power generation sectors [1]. Furthermore the upcoming Euro 6 emissions regulations which  
35 limit for the first time the particulate number have increased interest in the effect of  
36 oxygenated fuels on engine particulates; they have the potential to significantly reduce  
37 particulate emissions having health benefits, particularly for people living in urban areas [2,  
38 3]. The most commonly used biofuel component in spark ignition engines is ethanol;  
39 however there is increasing interest in the use of 1-butanol due to its higher calorific content,  
40 miscibility with gasoline, its water tolerance and its lower vapour pressure.

41  
42 Gumbleton et al. [4] investigated the effect of compression ratio on engine performance and  
43 emissions in six vehicles with medium sized PFI gasoline engines. They found that increased  
44 compression ratio improved specific fuel consumption; something which was also reported  
45 by Ref. [5], [6], [7] and [8-11]. This is most likely due to the improved thermal efficiency  
46 achieved with the higher compression ratio. However Ref. [9] reported that BSFC got worse  
47 under low-speed, high-load conditions at high compression ratios due to spark retardation  
48 caused by heavy knocking with low octane gasoline. Nevertheless improvements were  
49 observed when a high octane gasoline was used at increased compression ratios [9].

50  
51 Najafi et al. [12] investigated the effect of ethanol blended gasoline fuels on the performance  
52 and emissions of a 4-cylinder 1.3 litre SI engine. They observed that ethanol-gasoline

53 blended fuels increased the power (torque) of the engine across the engine load range because  
54 of the more advanced spark timings that could be achieved with ethanol blended fuel in  
55 comparison to gasoline. Ref. [13-17] reported similar findings. Brake specific fuel  
56 consumption improved; something which was attributed to the faster combustion of the  
57 ethanol fuel which increased the thermal efficiency of the engine. HC were observed to  
58 decrease with ethanol blending and  $\text{NO}_x$  was observed to increase. This was due to the  
59 enhanced oxidation and faster flame speed provided by the increased oxygen content of the  
60 ethanol fuel blend compared to gasoline. Ref. [13-15, 18-19] also observed HC emissions  
61 decrease with ethanol addition, however Ref. [20] observed no significant effect of ethanol  
62 blending on HC emissions. Ref. [14-15, 18-19, 21] observed  $\text{NO}_x$  emission decreases with  
63 ethanol addition, while Ref. [20] observed no significant effect of ethanol addition on  $\text{NO}_x$   
64 emissions. Perhaps this was due to the spark timing not being advanced when the ethanol-  
65 gasoline fuel blend was used.

66  
67 Deng et al. [22] studied the effect of 1-butanol blending on the performance and emissions of  
68 a single-cylinder PFI spark-ignition engine, using a 35%vol 1-butanol-gasoline blend; they  
69 compared this to a baseline of gasoline. They found that the ignition timing could be  
70 advanced with 1-butanol addition for higher thermal efficiency, due to the better knock  
71 suppression ability of 1-butanol fuel as compared to gasoline. The improved knock  
72 suppression ability has been attributed to the greater heat of vaporization of 1-butanol as  
73 compared to gasoline, giving it a greater charge cooling effect. Ref. [23-29] reported similar  
74 findings. Engine power (torque) and fuel consumption were found to have improved, with  
75 Ref. [25-26] and [28] reporting similar findings, due to the more advanced spark timings that  
76 could be achieved. Ref. [24], [26], [28] and [30-31] reported different findings however, with  
77 power and fuel economy observed to have decreased with increasing 1-butanol blended into

78 the gasoline fuel; most likely because the ignition timing was not advanced to its optimum  
79 point when the 1-butanol-gasoline fuel blend was used. Gu et al. [32] studied the emission  
80 characteristics of a 3-cylinder 0.8 litre PFI SI engine fuelled with 1-butanol-gasoline blended  
81 fuels; they found that 1-butanol addition to gasoline reduced the particle number  
82 concentration, due to the increased oxygen content of the 1-butanol fuel in comparison to  
83 gasoline. Ref. [23], [26] and [33-34] reported similar findings for butanol-gasoline blends.  
84 Ref. [23] reported that accumulation mode emissions showed the greatest reduction, most  
85 likely because these larger particles were more affected by the higher rate of oxidation  
86 achieved with the 1-butanol blended fuel, due to oxygen being present in its molecule.  
87 However Ref. [35] reported that 1-butanol addition increased the particle number  
88 concentration, which they attributed to poorer mixture formation.

89  
90 Maji et al. [13] investigated the effect of the compression ratio using ethanol-gasoline blends  
91 of 15 and 85%vol and a baseline fuel of gasoline on the performance and emissions of a  
92 single-cylinder PFI engine. They found that as the compression ratio was increased, the HC  
93 emissions increased for both gasoline and gasoline-ethanol blends; something which they  
94 attributed to the increased surface to volume ratio of the combustion chamber. Ref. [6-7] and  
95 [36] observed similar results with gasoline fuel; Ref. [7] attributed this to the higher relative  
96 influence of the crevice volume compared to the whole volume of the combustion chamber as  
97 well as in lower exhaust gas temperatures, supplying worse conditions for post-reactions of  
98 HC in the exhaust pipe as the compression ratio was increased. As discussed, HC emissions  
99 were also observed to have decreased with ethanol-gasoline fuel blends as compared to  
100 gasoline, due to the increased oxidization provided by the oxygen atom in the ethanol  
101 molecule.

102

103 Overall despite the amount of research that has been conducted into 1-butanol-gasoline and  
104 ethanol-gasoline blended fuels, there appears to be lack of agreement in terms of the effect  
105 these fuel blends on the combustion and emissions of gasoline engines. In addition, little  
106 work has been conducted regarding the effect of these fuel blends on the combustion and  
107 emissions of DISI engines with the majority of the research being conducted on PFI engines.  
108 Furthermore, 1-butanol-gasoline blended fuels have not been studied in detail in DISI  
109 engines, particularly their PM emissions. Finally, 1-butanol-gasoline and ethanol-gasoline  
110 fuel blends have not been studied well with each other along with a reference of gasoline fuel  
111 at different compression ratios. Therefore this research has been conducted to provide deeper  
112 knowledge about the effect of 1-butanol-gasoline and ethanol-gasoline blended fuels on  
113 combustion with focus on particulate matter (PM) emissions of DISI engines.

## 114 **2.0 Experimental Setup and Procedure**

### 115 **2.1 Engine and Instrumentation**

116 The specifications of the single cylinder DISI research engine used for the study are listed in  
117 Table 1, and the schematic is shown in Fig. 1. The engine was coupled to a direct current  
118 (DC) dynamometer and maintained at a constant speed of 1500 rpm ( $\pm 1$  rpm) regardless of  
119 the engine torque output. The in-cylinder pressure was measured using a Kistler 6041A  
120 water-cooled pressure transducer with a charge amplifier. Coolant and oil temperatures were  
121 maintained at 85°C and 95°C ( $\pm 3$ °C) respectively, using a proportional integral differential  
122 (PID) controller and heat exchangers. All temperatures were measured with K-type  
123 thermocouples. The compression ratio was modified by adjusting the number and size of the  
124 metal inserts placed beneath the cylinder head. These acted to adjust the height of the  
125 cylinder head in relation to the piston BDC allowing the compression ratio to be changed. A

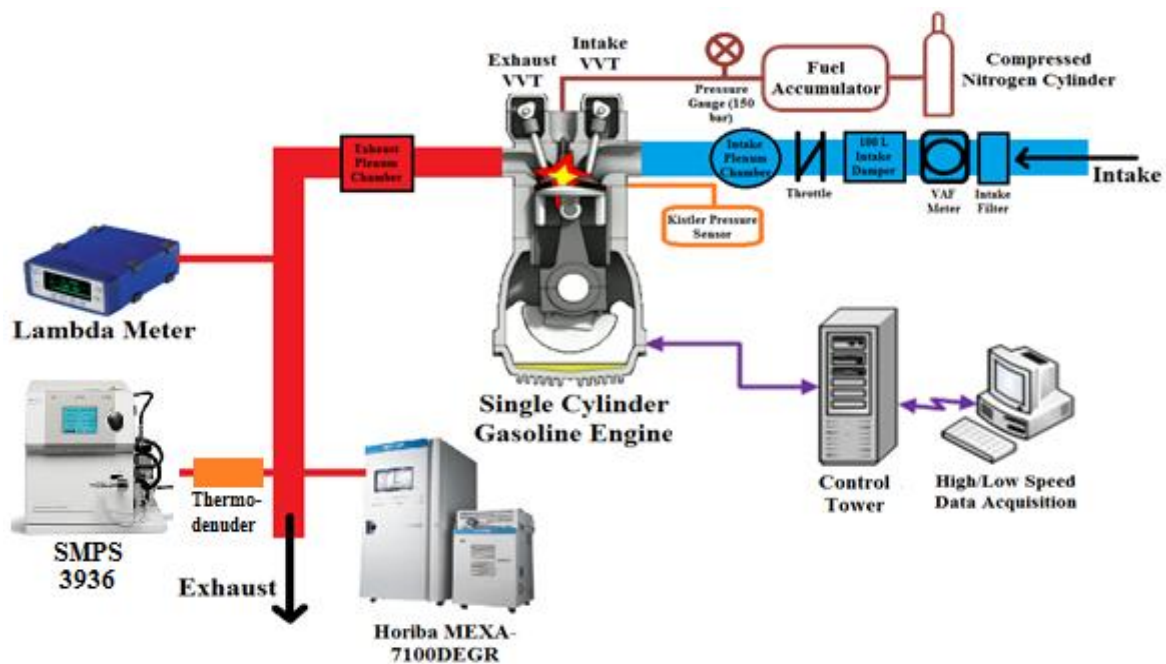
126 100 litre intake plenum tank (approximately 200 times the engine's swept volume) was used  
 127 to stabilize the intake air flow.

128 **Table 1** Experimental Single Cylinder Engine Specification

Parameter	
Engine Type	4-Stroke, 4-Valve
Combustion System	Spray Guided GDI
Swept Volume	565.6 cc
Bore x Stroke	90 x 88.9 mm
Engine Speed	1500 rpm
Engine Load	8.5 bar IMEP
DI Pressure and Injection Timing	15MPa, 280°bTDC*
Intake Valve Opening	16.0°bTDC**
Exhaust Valve Closing	36.0°aTDC**

\*TDC refers to TDC of combustion stroke, \*\*TDC refers to TDC of exhaust stroke.

129  
 130



131

132 **Fig. 1** Schematic of Engine and Instrumentation Setup [Colour website, B&W print]

133

134 Indicated fuel consumption was calculated from the measurement of the intake air flow rate  
 135 which was made using the volumetric air flow meter (VAF). The load of 8.5 bar IMEP was  
 136 chosen to study because it represents one of the worst conditions for engine knock in this

137 naturally aspirated (NA) engine, as well as being an engine load that is highly relevant for  
138 both NA and turbocharged DISI engines, increasing the usefulness of the data produced.

139  
140 The engine cylinder head was a single-cylinder version of that used in the 2010 Jaguar  
141 LandRover AJ133 5.0 litre V8 engine. It was mounted on a modified single cylinder research  
142 engine and was not designed to be very resistant to knock. The engine has been used in this  
143 study for investigation of engine knocking phenomena. Therefore engine knock occurred at  
144 loads of 6.0 bar IMEP and above, which is somewhat lower than what can be expected with  
145 the state of the art aggressively downsized engines of modern cars on sale today.  
146 Furthermore, audible knock was observed to start occurring with 97 RON gasoline fuel at  
147 engine loads between 4.5 and 6.0 bar IMEP by previous researchers using this research  
148 engine [37-40]. Therefore the occurrence of knock at loads of 6.0 bar IMEP and above is  
149 consistent with these previous investigations.

150  
151 The engine was controlled by an in-house program written in LabVIEW. All the engine  
152 operating data, pressure, and temperature data were acquired using another in-house  
153 LabVIEW program. For PM collection, the exhaust samples were taken 300 mm downstream  
154 of the exhaust valve of the engine, as indicated in the figure. They were then diluted by air  
155 (dilution ratio 4:1) at 150°C to avoid condensation of the particulates, passed through a Topas  
156 TDD 590 thermodenuder at a temperature of 400°C to remove most of the volatile nucleation  
157 mode particles and analysed in the Scanning Mobility Particle Sizer Spectrometer  
158 (SMPS3936) manufactured by TSI. The exhaust temperature at the sampling point was above  
159 150°C at all times, so that the particulates did not condense before they were sampled. For  
160 NO<sub>x</sub> and HC emission measurement, the exhaust samples were taken opposite the PM sample  
161 point using the Horiba sampler device before being pumped via a heated line maintained at



162 190°C to the Horiba MEXA7100EGR emissions measurement system, where they were  
163 subsequently analysed.

164  
165 A Labview program was developed in order to remove the unwanted noise from the pressure  
166 trace, to identify the knocking amplitude. The program read the on-line pressure data and  
167 applied a Butterworth second order type filter to isolate the frequency range of 4-12Hz,  
168 which ensured that the first and second harmonic knocking frequencies from the engine  
169 remained after the low and high frequency engine – generated signal noise had been  
170 removed. It then calculated the knocking amplitude from the amplitude of the filtered  
171 pressure trace. This provided on-line knocking amplitudes which allowed the KLMBT spark  
172 timing to be quantified at each engine condition before the engine data was recorded. The  
173 KLMBT was defined as the most advanced spark timing with 97% or more of the cycles  
174 having knock amplitudes below 2 bar. The maximum acceptable knock amplitude of 2 bar  
175 was chosen based on the work of Mittal et al. in Ref. [41]. If the maximum brake torque had  
176 been reached before the KLMBT timing, then this spark timing was defined as the KLMBT.  
177 Another in-house MatLab script was used to analyse the in-cylinder pressure trace along with  
178 other relevant parameters in order to calculate the MFB inside the combustion chamber; the  
179 same script was used in a previous publication by this research group [42].

180  
181 The theoretical average in-cylinder temperatures were calculated using a detailed engine gas-  
182 dynamics and thermodynamics model used by the authors' research group in Ref. [1] and  
183 described in [37]. The model provides a good correlation between its simulated outputs and  
184 the experimental data. Fundamental assumptions made in the model are based on the  
185 information provided by Heywood [43]. Rather than using a relatively complex chemical  
186 kinetics model, the ideal gas law was used and combined with the prediction of trapped  
187 residuals and fuel vaporization behaviour to estimate the average in-cylinder gas temperature.

188 When simulating the combustion of gasoline, the fluid properties of indolene were used.  
189 When simulating the combustion of the fuel blends used, the known properties were inputted  
190 A primary combustion sub-model based on the recorded mass fraction burned (MFB) profile  
191 was used along with a SI Wiebe combustion sub-model which required the input of MFB50  
192 and MFB10-90, in order to simulate the in-cylinder temperature conditions. In addition, a  
193 secondary sub-model was used based on the recorded pressure data to further enhance its  
194 precision. The model was validated using known combustion performance data to maintain  
195 the volumetric efficiencies to within 5% at all tested engine loads.

## 196 **2.2 Test Fuels**

197 The properties of the three studied fuels are listed in Table 2. Both gasoline and ethanol were  
198 supplied by Shell Global Solutions, UK. The 1-butanol was supplied by Fisher Scientific UK  
199 Ltd. The ULG95 was used in its supplied form, while the 1-butanol and ethanol fuels were  
200 mixed with the ULG95 fuel to form the Bu20 and E20 fuel blends with each containing  
201 20%vol 1-butanol and 20%vol ethanol respectively. The ULG95 fuel was supplied with  
202 5%vol ethanol pre-mixed in it, so the 20%vol 1-butanol blend and ULG95 fuel also had  
203 5%vol ethanol in them too, while the 20%vol ethanol blend did not have any additional  
204 ethanol. It was chosen to study ethanol blended into gasoline fuel rather than in its pure form  
205 because ethanol is used on a wide scale only in its blended forms of up to 20%vol and in the  
206 near future this trend is likely to continue with ethanol-gasoline blends between 20-40%vol  
207 [20]. Therefore the blended form was tested which will not only allow the effect of ethanol  
208 addition to gasoline on DISI engine performance and emissions to be quantified, it will allow  
209 the precise effects of one of the most relevant ethanol-gasoline blends on DISI engine  
210 performance and emissions to be quantified. 1-butanol while not widely used in 1-butanol-  
211 gasoline blends has the potential to be used in the future with similar blend ratios as ethanol-  
212 gasoline blending; therefore 1-butanol has also been studied. It was studied in its Bu20 blend

213 with gasoline rather than its pure form due to the same reason ethanol was studied in its  
 214 blended form.

215 **Table 2** Test Fuel Properties

Parameter	Butanol	Ethanol	ULG95	Bu20	E20
Chemical Formula	C <sub>4</sub> H <sub>10</sub> O	C <sub>2</sub> H <sub>6</sub> O	C <sub>2</sub> -C <sub>14</sub>	C <sub>2</sub> -C <sub>14</sub>	C <sub>2</sub> -C <sub>14</sub>
H/C Ratio	2.5	3	1.922	2.038	2.084
O/C Ratio	0.25	0.5	0.021	0.067	0.093
Gravimetric oxygen content (%)	21.6	34.78	2.36	6.21	8.84
Density @ 20°C (kg/m <sup>3</sup> )	811	790.9*	743.9	757.3	753.3
Research Octane Number (RON)	98	106	95	-	102 [44]
Stoichiometric air-fuel ratio	11.2	8.95	14.15	13.71	13.78
LHV (MJ/kg)	32.71	26.9*	42.22	39.73	37.76
Initial boiling point, IBP (°C)	118	78.4	34.6	34.6	34.6
Heat of Vaporization $\Delta_{\text{vap}}H$ (@ IBP) (kJ/kg)	585	858	373	-	-

216 \* Measured at the University of Birmingham.

217  
 218 **2.3 Experimental Procedure**

219 The engine was considered warmed-up once the coolant and lubricant temperatures were  
 220 stabilized at 85°C and 95°C respectively, and once the engine cylinder block had been  
 221 warmed to 95°C, as measured by a thermocouple embedded 5 mm within the block. Tests  
 222 were carried out at ambient air intake conditions (approximately 25°C). Indicated engine  
 223 loads were controlled by adjusting the throttle position and injection duration. Relative air-  
 224 fuel ratio  $\lambda$  was maintained at 1 during the experiments and a 5% COV of the IMEP was not  
 225 exceeded. Once the engine load condition had been achieved, 300 pressure cycles along with  
 226 engine emissions and particulate data were recorded. This procedure was then repeated for  
 227 the different engine fuel blends and reference fuel, and then again for the different  
 228 compression ratios. The test matrix for this investigation shown in Table 3 comprised an  
 229 overall number of 12 measurements. Readings for each measurement were taken  
 230 consecutively until 3 consistent readings were recorded. For the data presented in Fig. 3 and  
 231 6, the averaged data from the 3 readings was plotted along with the 95% confidence intervals,

232 in order to enable the significant effects of compression ratio and fuel on the data to be  
 233 identified. The confidence intervals were calculated using equation (1).

234 
$$CI = \bar{x} \pm Z_{\alpha/2} * \frac{\sigma}{\sqrt{n}} \quad (1)$$

235 where CI = confidence interval,  $\bar{x}$  = mean,  $Z_{\alpha/2}$  = factor based on the desired confidence  
 236 interval of 95%, which is 1.96,  $\sigma$  = standard deviation and n = sample size.

237 **Table 3** Experiment Test Matrix

Compression Ratio	10.7	10.9	11.2	11.5
Fuel				
<b>Bu20</b>	1	2	3	4
<b>E20</b>	5	6	7	8
<b>ULG95</b>	9	10	11	12

238

### 239 **3.0 Results and Discussion**

#### 240 **3.1 KLMBT Spark Timing**

241

242 From the knock limited maximum brake torque (KLMBT) spark timings in Table 4, it can be  
 243 seen that in the case of gasoline, an increase in the compression ratio had no significant effect  
 244 on KLMBT. The same trend is also obtained for the butanol blend (similar octane rating than  
 245 gasoline) and even for the ethanol blend, despite the high octane rating of ethanol. This is  
 246 because at the engine load of 8.5 bar IMEP, the engine was very prone to knock, even in the  
 247 case of alcohols, due to the high low temperature reactivity of alcohols [44] and the higher  
 248 amount of fuel being injected into the combustion chamber (i.e. ethanol has lower calorific  
 249 value than butanol and gasoline). Thus despite the compression ratio changing, no change in  
 250 the KLMBT spark timing could be realized.

251 It can also be seen that more advanced KLMBT spark timings could be achieved with Bu20  
 252 and E20 as compared to ULG95, with the most advanced spark timings being achieved with  
 253 Bu20. This is due to their higher octane number and the superior charge cooling effect of

254 alcohols compared to gasoline. Despite ethanol having a higher octane number than 1-butanol  
 255 and cooling effect (in terms of mass), a more advanced KLMBT spark timings could be  
 256 achieved with Bu20. It is believed that the 5% vol ethanol content in the Bu20 blend (20% vol  
 257 1-butanol with 5% vol ethanol) was sufficient to compensate for the lower charge cooling and  
 258 octane number effect of 1-butanol as compared to ethanol. It is also thought that the higher  
 259 chemical reactivity [44], faster laminar flame speeds and shorter fuel injection duration (less  
 260 fuel quantity is required for the same engine output power due to the higher heating value  
 261 than ethanol) for the butanol blend with respect to ethanol blend meant that the end-zone  
 262 auto-ignition sites were consumed before they had an opportunity to auto-ignite, thus also  
 263 contributing to the KLMBT spark advances.

264

**Table 4 KLMBT Spark Timings (°bTDC)**

<b>Compression Ratio</b>	<b>10.7</b>	<b>10.9</b>	<b>11.2</b>	<b>11.5</b>
<b>Fuel</b>				
<b>Bu20</b>	14°	14°	14°	14°
<b>E20</b>	12°	12°	12°	12°
<b>ULG95</b>	10°	10°	10°	10°

265

### 266 **3.2 In-Cylinder Pressures and Temperatures, and Mass Fraction Burned** 267 **(MFB)**

268

269 The in-cylinder pressure traces for the two fuels blends of Bu20 and E20 along with that for  
 270 the ULG95 reference fuel are shown in Fig. 2a, 2b, and 2c respectively. It is clear that as the  
 271 compression ratio was increased, the maximum in-cylinder pressure increased, for the two  
 272 fuel blends and the reference fuel tested. This is because the more compact combustion  
 273 chamber achieved through the compression ratio increase, reduced the heat losses to the  
 274 surroundings, resulting in the in-cylinder pressure increases. The in-cylinder pressures were  
 275 highest for Bu20, followed by E20, then ULG95. This is due to the more advanced KLMBT  
 276 spark timings which could be achieved with Bu20 and E20 as compared to those achieved

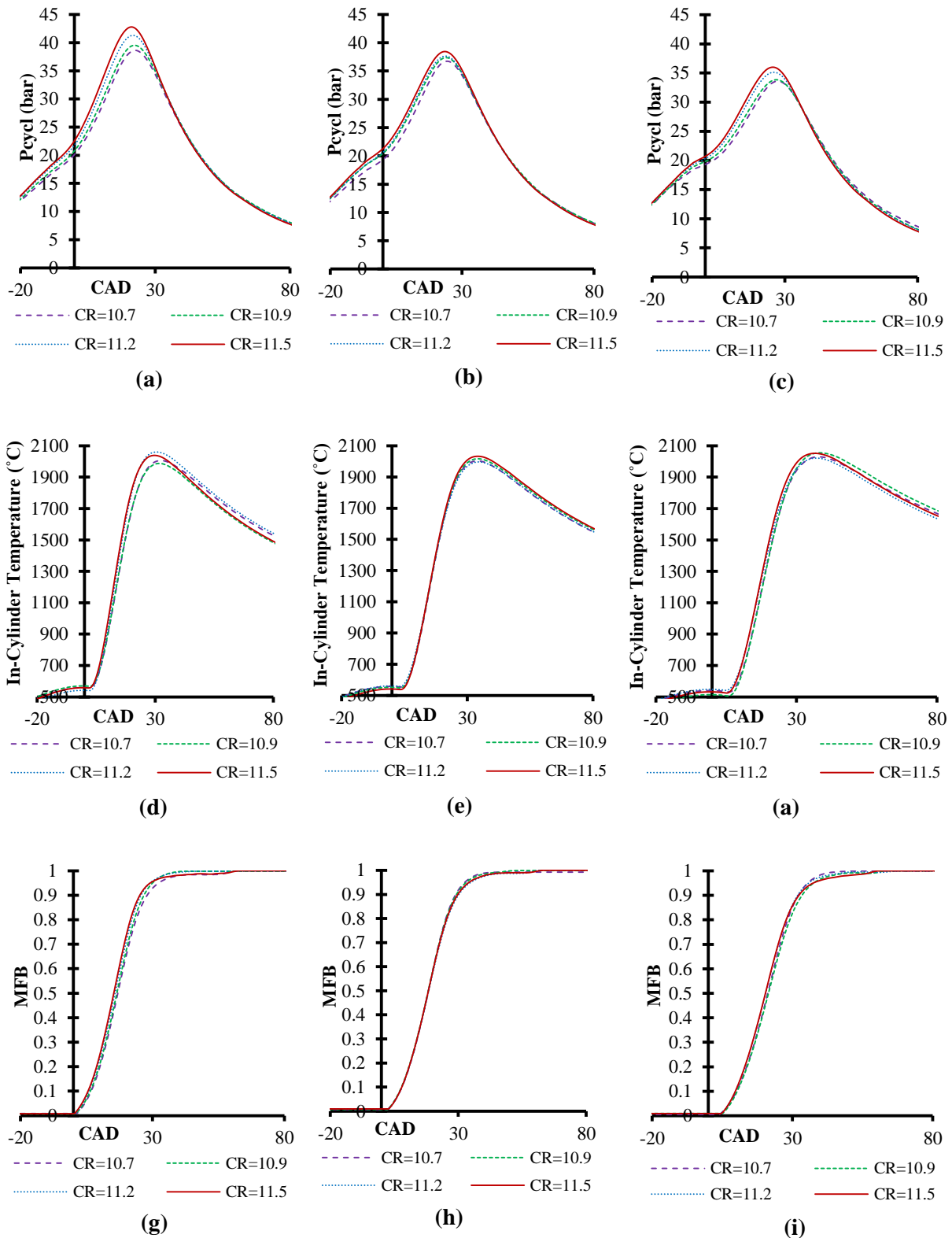
277 with ULG95, with the most advanced spark timings being achieved for Bu20; these are  
278 shown in Table 4. This made the combustion quicker and more efficient as the MFB50 point  
279 was advanced towards its optimum 8-10°aTDC phase [45], as shown in Fig. 3a, resulting in  
280 the higher in-cylinder pressures observed.

281  
282 Fig. 2d, 2e and 2f show the calculated average in-cylinder temperatures for the two fuel  
283 blends of Bu20 and E20 and for the reference fuel of ULG95, respectively. Overall the  
284 calculated average in-cylinder temperature increased as the compression ratio was increased.  
285 This is because of the aforementioned increase in in-cylinder pressure which resulted from  
286 the more compact combustion chamber achieved with the compression ratio increase. The  
287 calculated average in-cylinder temperatures were highest for ULG95, with Bu20 and E20  
288 having lower but similar calculated average in-cylinder temperatures across the compression  
289 ratio range. It is proposed that this is due to the higher heat of vaporization of 1-butanol and  
290 ethanol as compared to ULG95, as shown in Table 2. This meant that more energy was  
291 required to vaporize these fuels, causing the average in-cylinder temperatures to reduce. The  
292 earlier start of combustion (advanced KLMBT and higher chemical reactivity) and especially  
293 the quicker combustion speed of butanol with respect to ethanol also contributed to the lower  
294 average in-cylinder temperatures.

295  
296 The MFB profiles for the two tested fuel blends of Bu20 and E20, and the reference fuel of  
297 ULG95 are shown in Fig. 2g, 2h and 2i, respectively. For E20 there are no significant  
298 differences between the profiles at the different compression ratios while Bu20 and ULG95  
299 show a slightly advanced combustion as the compression ratio was increased. It is proposed  
300 that the more highly compressed fuel-air mixture at the higher compression ratio burned more  
301 quickly than the less highly compressed mixtures at the lower compression ratios, causing the  
302 combustion to proceed more quickly. Despite this, it appears that the last stage of combustion

303 (less than 10% of the fuel mass remaining) was faster at lower compression ratios for all three  
304 fuels. For a quantitative analysis of the combustion speed MFB10, MFB50 and MFB90 has  
305 been calculated from the MFB profiles (please see next section).

306



307 **Fig. 2** In-Cylinder Pressures versus CAD for a) Bu20, b) E20 and c) ULG95 at KLMBT spark timings;  
 308 calculated (estimated) average In-Cylinder Temperatures versus CAD at KLMBT spark timings for d) Bu20, e)  
 309 E20 and f) ULG95; MFB versus CAD at KLMBT spark timings for g) Bu20, h) E20 and i) ULG95 [Colour  
 310 website, B&W print]



### 311 **3.3 MFB50, MFB10-90, Exhaust Gas Temperature and Indicated** 312 **Efficiency**

313  
314 Fig. 3a shows the MFB50 data for the two tested fuel blends of Bu20 and E20, and the tested  
315 reference fuel of ULG95, across the compression ratio range. As discussed and explained  
316 previously, the KLMBT spark timings were most advanced for Bu20, with E20 second and  
317 ULG95 third, thus leading to the most advanced MFB50 of Bu20 across the compression  
318 ratio range, followed by E20 and ULG95. The MFB50 remained almost constant across the  
319 compression ratio range for E20; this is reflected in the MFB profile for E20 presented in Fig.  
320 2h. However for the other two fuels of B20 and ULG95, there was a significant reduction in  
321 the MFB50 across the compression ratio range.

322  
323 Fig. 3b shows the MFB10-90 data for the two tested fuel blends of Bu20 and E20, and the  
324 tested reference fuel of ULG95, across the compression ratio range. 1-butanol and ethanol  
325 addition to gasoline reduced the combustion duration of the fuel; it is proposed that 1-butanol  
326 and ethanol increased the linear flame speed, due to the oxygen in their molecule. The higher  
327 chemical reactivity of 1-butanol as compared to ethanol and the shorter injection duration of  
328 Bu20 with respect to E20 explains its shorter combustion duration in comparison. It has to be  
329 also noted that the combustion duration of Bu20 reduced significantly across the compression  
330 ratio range; this continues the trend in Fig. 3b which shows that the first half of the  
331 combustion process also proceeded more quickly across the range.

332  
333 Fig. 3c shows the exhaust gas temperatures for the two tested fuel blends of Bu20 and E20,  
334 and the tested reference fuel of ULG95 across the compression ratio range. It is clear to see  
335 that there is general small decrease in exhaust gas temperatures across the compression ratio  
336 range. It is proposed that as the compression ratio increased and the MFB50 became  
337 advanced to its optimum 8-10°aTDC CA50 point [45], the pressure and heat was more  
338 efficiently converted into work on the piston leading to the exhaust gas temperature decreases

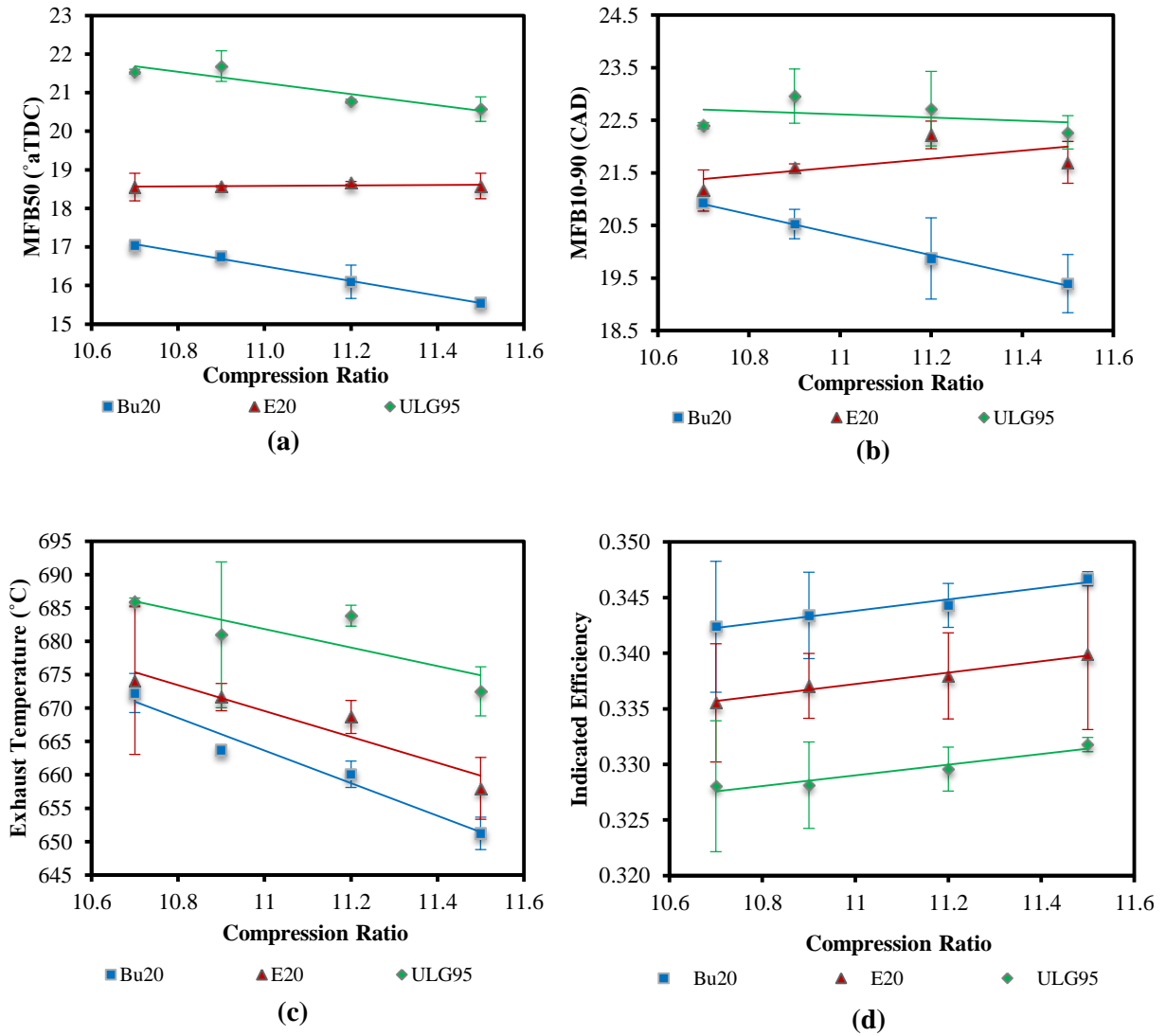
339 across the compression ratio range [20]. Ref. [7] also observed exhaust gas temperature  
340 reductions as compression ratio was increased. The results also show that ULG95 had the  
341 highest exhaust gas temperature for all compression ratios, followed by E20, then Bu20. It is  
342 proposed that the more advanced MFB50 point of Bu20 as compared to ULG95 and E20  
343 shown in Fig. 3a resulted in more efficient conversion of the pressure and heat into work on  
344 the piston, resulting in the reduced exhaust gas temperatures in comparison. Also as shown in  
345 Fig. 3a, the MFB50 point was more advanced for E20 than ULG95 for all compression ratios  
346 leading to lower exhaust gas temperatures in comparison, again due to more efficient  
347 conversion of the pressure and heat into work on the piston. The lower calculated average in-  
348 cylinder temperatures for the Bu20 and E20 fuel blends due to their higher heat of  
349 vaporization as compared to ULG95, will have also contributed to their lower exhaust gas  
350 temperatures, in comparison.

351  
352 The indicated efficiency for the two tested fuel blends of Bu20 and E20, and the tested  
353 reference fuel of ULG95, across the compression ratio range, is shown in Fig. 3d. This was  
354 quantified by calculating the work output from the engine, then dividing it by the heat input  
355 from the fuel. They increased by 1.26%, 1.30% and 1.14% for Bu20, E20 and ULG95,  
356 respectively. This compares to a maximum theoretical thermal efficiency increase of 1.80%  
357 which can be obtained from equation (2) by assuming  $\gamma=1.4$  and solving for the minimum  
358 and maximum respected compression ratios of 10.7 and 11.5.

359 
$$n_{th=1} = 1 - \frac{1}{r^{\gamma-1}} \quad (2)$$

360 Therefore the thermal efficiency increase observed is realistic. As the compression ratio is  
361 increased, indicated (thermal) efficiency increases, thus producing the observed behaviour.  
362 Bu20 had the highest indicated efficiency, followed by E20 then ULG95, due to their  
363 respected KLMBT spark timings (Table 4) and their respected combustion durations (Fig.

364 3b). The more advanced the spark timing and the faster the combustion, the more efficiently  
 365 the fuel was converted into engine power, thus resulting in the indicated efficiency increases  
 366 observed.



367 **Fig. 3** Combustion parameters versus Compression Ratio at KLMBT spark timings a) MFB50, b) MFB10-90, c)  
 368 exhaust Temperature, d) indicated Efficiency [Colour website, B&W print]  
 369

370

371

## 372 **3.4 PM Emission Characteristics**

### 373 **3.4.1 Compression Ratio Effect on PM Number Emission**

374 The particulate matter number emissions for the two tested fuel blends of Bu20 and E20,  
375 along with the tested reference fuel of ULG95 are shown in Fig. 4a, 4b and 4c, respectively.  
376 It is clear to see from Fig. 4a that compression ratio increase reduced the smaller nucleation  
377 mode particles on the left-hand side of the plot (3-30nm) for Bu20 blend. According to Ref.  
378 [24], the nucleation mode particles mainly result from droplets formed by hydrocarbon  
379 condensation and the accumulation mode particles are mainly composed of carbonaceous  
380 agglomerates formed in local rich-fuel zones [46, 47]. It is proposed the observed reduction  
381 was due to the increased calculated average in-cylinder temperatures across the compression  
382 ratio range which increased the oxidation of the particles in the combustion chamber. The  
383 KLMBT spark timing was unchanged across the compression ratio range, therefore mixture  
384 preparation was not considered to have had an effect on the observed behaviour.

385  
386 E20 showed a similar trend to Bu20 but it was much weaker; the nucleation mode particles  
387 decreased as the compression ratio was increased. Again it is proposed that the higher  
388 calculated average in-cylinder temperatures shown in Fig. 2e increased the rate of oxidation  
389 of these particles in the combustion chamber, leading to the observed trend. For both Bu20  
390 and E20 no significant changes in accumulation mode particle numbers were observed. It is  
391 believed that the increased oxidization of particles resulting from the increased calculated  
392 average in-cylinder temperatures across the compression ratio range was cancelled out by  
393 increased rate of particle formation caused by the increase in primary carbon particle  
394 formation by thermal pyrolysis and dehydrogenation reactions [23], also resulting from the  
395 increased calculated average in-cylinder temperatures.

396 The data for ULG95 shows a completely uni-modal distribution with no significant  
397 nucleation mode particles being recorded. As the compression ratio was increased, the  
398 formation of accumulation mode particles on the right hand side of the plot (30-500nm)  
399 increased. It is proposed that the accumulation mode particles increased across the  
400 compression ration range for ULG95 because the increased calculated average in-cylinder  
401 temperatures increased the particle formation rate, as with E20 and Bu20. This appears to  
402 have overcome the effect of increased particle oxidization resulting from the higher  
403 calculated average in-cylinder temperatures. Again the KLMBT spark timing was unchanged  
404 across the compression ratio range, thus mixture preparation is not thought to have had an  
405 effect on the observations.

406  
407 For the two tested fuel blends Bu20 and E20, along with the tested reference fuel ULG95, it  
408 is proposed that significant nuclei adsorption of nucleation particles onto the accumulation  
409 particles occurred and this along with the thermodenuder, which removed many of the  
410 nucleation particles before they could be measured, lead to the mostly uni-modal behaviour  
411 observed.

### 412 3.4.2 Fuel Effect on PM Number Emission

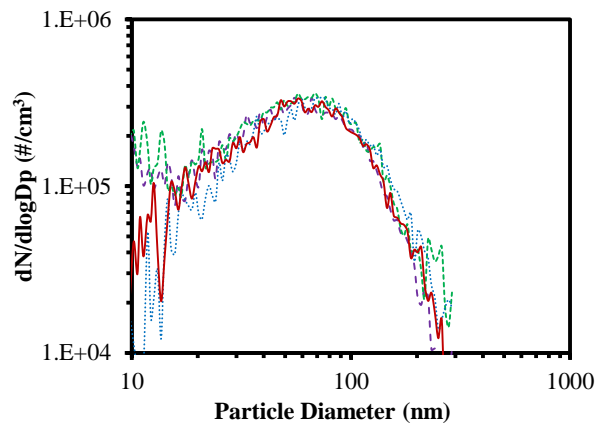
413 Comparing the behaviours of the different fuels in Fig. 4a, 4b and 4c, 1-butanol significantly  
414 reduced the particle number when added to the gasoline fuel, whereas ethanol had little or no  
415 effect. It is proposed that the significantly earlier MFB50 point and shorter combustion  
416 duration of Bu20 as compared to the other two fuels provided more time for oxidation of the  
417 particulates after the combustion process, leading to the significant particle number reduction.  
418 This appears to have overcome the advanced KLMBT spark timing, which may have  
419 provided benefits in increased post-combustion oxidation time, but, on the other hand, would  
420 have reduced the fuel-air mixing time; and reduced calculated average in-cylinder  
421 temperatures. These would have resulted in more areas with a high local equivalence ratio  
422 and a reduced oxidation rate in the combustion chamber, respectively, which alone would  
423 have led to an increase in accumulation mode particles. However the increased post-  
424 combustion oxidization time was clearly the stronger effect. Also it is important to note that  
425 reduced calculated average in-cylinder temperatures will have also reduced the soot  
426 formation rate through reducing the primary carbon particles formed by thermal pyrolysis and  
427 dehydrogenation reactions; thus this may have contributed to the reductions observed. In  
428 addition, it is thought that because the gasoline already had 5%vol ethanol content, the  
429 increase in ethanol content to 20%vol made little difference to the particle number behaviour.

430  
431 Overall there is no significant effect of fuel type on the particles average size with all  
432 distributions peaking at around 60nm. Ref. [23], [26] and [32-34] also reported that 1-butanol  
433 addition to gasoline fuel reduced the particle number concentration, and Ref. [18-19] and [48-  
434 53] also observed the same for ethanol addition to gasoline fuel.

435

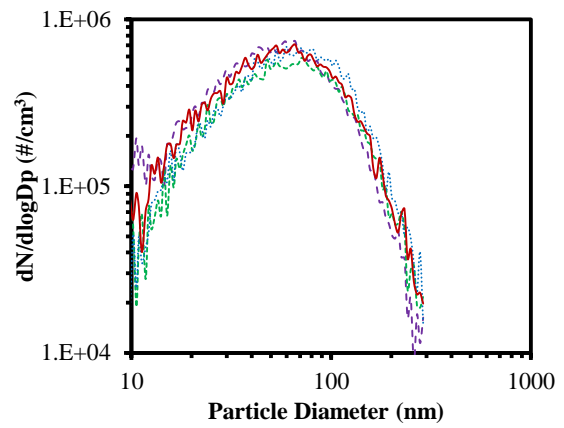
436 There are further reasons as to why the accumulation mode particles decreased with butanol  
437 addition to gasoline fuel. Firstly, the reduced calculated average in-cylinder temperatures  
438 caused the primary carbon particles formed by thermal pyrolysis and dehydrogenation  
439 reactions to decrease [23]. Secondly, there is a positive correlation between the accumulation  
440 mode particles and the polycyclic aromatic hydrocarbon (PAHs); the addition of alcohol to  
441 gasoline reduces the aromatic content of the fuel, thus it also caused the accumulation mode  
442 particles to decrease [23]. Thirdly, the oxygen content in the fuel blend leads to a lower  
443 formation rate of soot and also to a higher oxidation rate of soot [23]. Despite these reasons  
444 contributing significantly to the reduction in accumulation mode particles observed for the  
445 Bu20 fuel blend, they did not decrease significantly for the E20 fuel blend in comparison to  
446 the reference ULG95 fuel. Lastly, Bu20 had a noticeably higher number of nucleation mode  
447 particles than the other two fuels tested. It is thought that this was due to the lower soot  
448 accumulation mode particles observed, which meant less adsorption of the nucleation mode  
449 particles onto the accumulation mode particle surfaces occurred, leading to higher numbers  
450 being observed in comparison to E20 and ULG95.

451  
452 Overall, the effect of 1-butanol addition to gasoline on PM emissions is significant when the  
453 95% confidence intervals are taken into consideration, while ethanol addition to gasoline has  
454 no significant effect at the blend ratio tested. Fig. 5 provides a summary of the effects of  
455 compression ratio and fuel on PM number emissions.



- - - CR=10.7      - - - CR=10.9  
 ····· CR=11.2      ——— CR=11.5

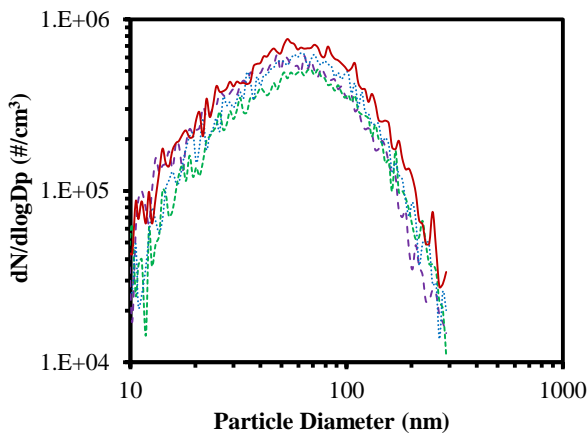
(a)



- - - CR=10.7      - - - CR=10.9  
 ····· CR=11.2      ——— CR=11.5

(b)

456



- - - CR=10.7      - - - CR=10.9  
 ····· CR=11.2      ——— CR=11.5

(c)

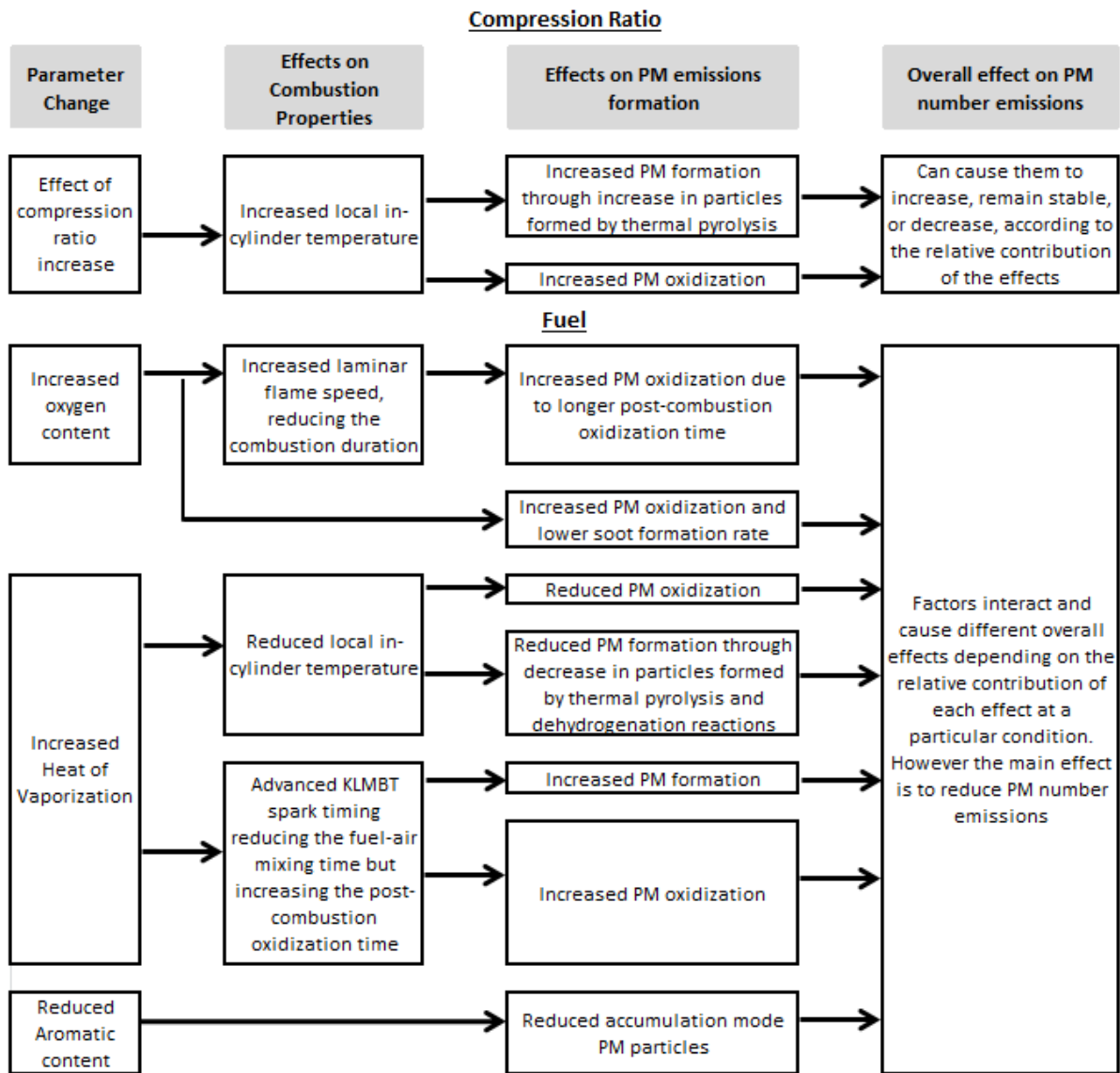
457

458

459

**Fig. 4** PM number emissions at KLMBT spark timings for **a)** Bu20, **b)** E20 and **c)** ULG95 [Colour website, B&W print]





460

461 **Fig. 5** Summary of the effects of compression ratio and fuel on PM number emissions [B&W website, B&W  
462 print]

463

### 464 3.5 NO<sub>x</sub> and HC emissions

465

466 Fig. 6a presents the NO<sub>x</sub> emission data for the two tested fuel blends and tested reference

467 fuel. Overall there is a significant increase in NO<sub>x</sub> emissions across the compression ratio

468 range; they increased by 17.38% for Bu20, 21.69% for E20, and 23.51% for ULG95. These

469 increases occurred because of the aforementioned increase in in-cylinder temperatures across

470 the compression ratio range, which caused more NO<sub>x</sub> to be formed. It is also clear that

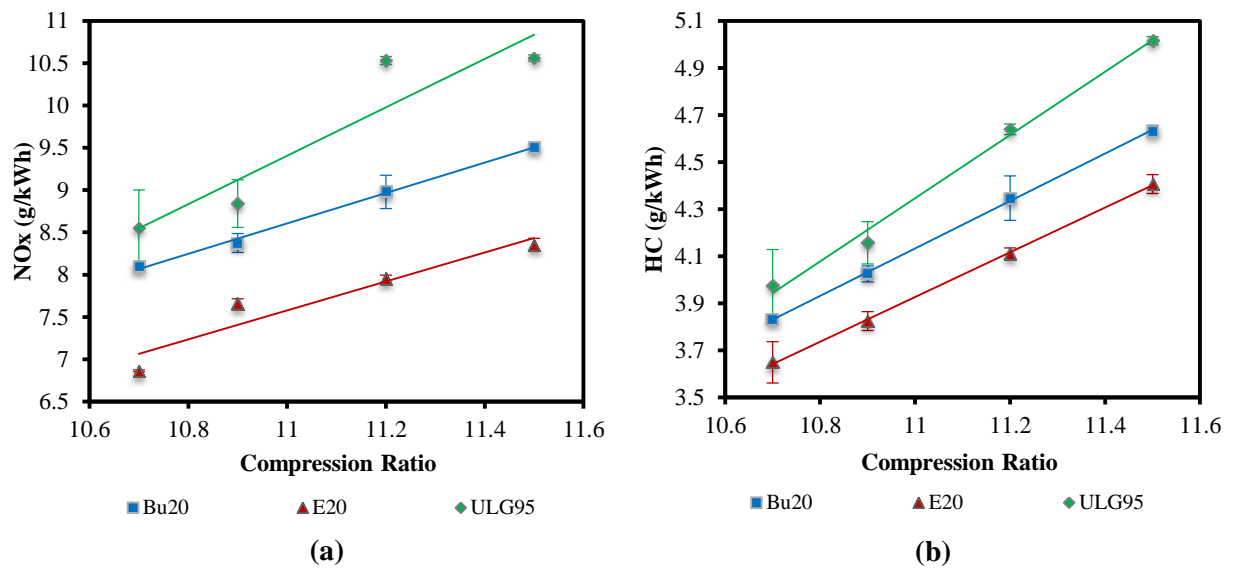
471 ULG95 had the highest NO<sub>x</sub> emission, followed by Bu20 then E20. It is proposed that the

472 lower calculated average combustion temperatures of Bu20 and E20 as shown in Fig. 2d and

473 2e, respectively, reduced the formation of  $\text{NO}_x$  emissions. Despite the calculated average in-  
474 cylinder temperatures being similar for Bu20 and E20 across the compression ratio change  
475 and ethanol having a higher O/C ratio than 1-butanol, Bu20 produced more  $\text{NO}_x$  emissions  
476 than E20. It is proposed that the earlier MFB50 of Bu20 as compared to E20, as shown in  
477 Fig. 3a, provided more time for  $\text{NO}_x$  to form in the hot flames, causing the higher  $\text{NO}_x$   
478 emissions in comparison.

479  
480 Fig. 6b presents the HC emissions data for the two tested fuel blends and the tested reference  
481 fuel. It is clear to see that the HC emissions increased significantly across the compression  
482 ratio range; they increased by 20.9% for Bu20, 20.8% for E20 and 26.2% for ULG95. It is  
483 suggested that the increased surface to volume ratio of the combustion chamber and the  
484 higher relative influence of the crevice volume as compared to the whole volume of the  
485 combustion chamber resulted in the observed HC emission increases [7, 13].

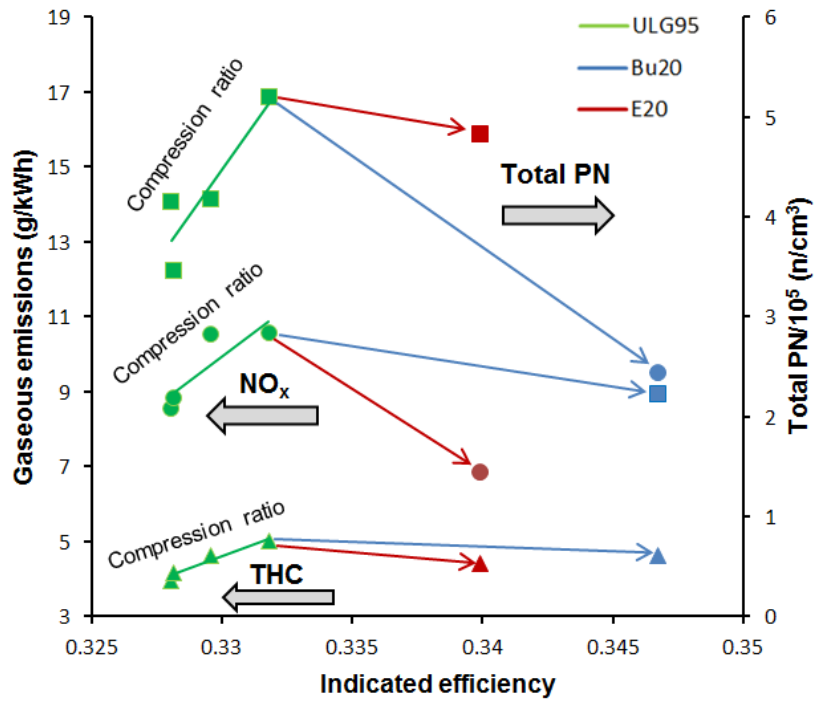
486  
487 The emissions were lower for Bu20 and E20 as compared to ULG95 because their oxygen  
488 content was higher, which promoted the oxidation of HC in the combustion chamber. This  
489 appears to have overcome the reduced fuel-air mixing time caused by the more advanced  
490 KLMBT spark timing and the reduced combustion temperatures, which alone will have  
491 caused the HC emissions to increase. Ethanol has a higher oxygen to carbon ratio than 1-  
492 butanol, thus there was a higher HC oxidation rate of E20 as compared to Bu20, leading to  
493 lower HC emissions in comparison. Also the KLMBT spark timing was more advanced for  
494 the Bu20 fuel blend in comparison to E20, resulting in poorer mixture preparation and thus  
495 higher HC emissions. Finally the in-cylinder pressures were higher for Bu20 leading to more  
496 HCs being stored in the piston crevice area, contributing to the higher HC emissions observed  
497 for the Bu20 fuel blend.



498 **Fig. 6** Gaseous emissions versus Compression Ratio at KLMBT spark timings **a)** NO<sub>x</sub>, **b)** HC [Colour website,  
 499 **B&W print]**  
 500  
 501

### 502 **3.6 Big Picture**

503 Fig. 7 shows the overall effect of compression ratio and fuel on the gaseous emissions,  
 504 indicated efficiency and total PN, while Fig. 8 summarises the compression ratio and fuel  
 505 pathways affecting the combustion process, fuel economy and gaseous and particulate matter  
 506 emissions. It is clear to see that for ULG95, the gaseous emissions of NO<sub>x</sub> and HC increased  
 507 with increased compression ratio, along with the indicated efficiency and total PN. However,  
 508 when 1-butanol and ethanol are blended into the ULG95 fuel, the gaseous emissions of NO<sub>x</sub>  
 509 and HC are reduced, along with total PN, and the indicated efficiency is increased. Ethanol is  
 510 most effective to reduce the gaseous emissions of NO<sub>x</sub> and HC of the ULG95 fuel and 1-  
 511 butanol is most effective to reduce the total PN emission.  
 512



513

514 **Fig. 7** Overall effect of compression ratio and fuel on gaseous emissions, indicated efficiency and total PN  
 515 (integrated across 10-289nm range) at KLMBT spark timings [Colour website, B&W print]

516

517

518 **4.0 Conclusions**

519

520 The effect of compression ratio and fuel on combustion and PM emissions in a single  
521 cylinder DISI research engine was investigated in this paper and the following conclusions  
522 have been made.

523 **1.** 1-butanol and ethanol addition to gasoline advanced the MFB50 point as well as reducing  
524 the overall combustion duration across the compression ratio range; 1-butanol had the  
525 greatest effect on these parameters.

526 **2.** 1-butanol addition to gasoline significantly reduced the accumulation mode particulate  
527 number emission, due to the earlier combustion phasing and thus increased post-  
528 combustion oxidization time; ethanol addition to gasoline had little effect on the  
529 emission.

530 **3.** 1-butanol and ethanol addition to gasoline significantly reduced the NO<sub>x</sub> and HC  
531 emission across the compression ratio range, with ethanol being the most effective.

532 **4.** Overall, if combustion and PM number emission parameters are the priority, then the  
533 Bu20 fuel blend has the most potential, while if NO<sub>x</sub> and HC emission parameters are the  
534 priority, then the E20 fuel blend has the most potential. Synergies between compression  
535 ratio increase and alcohol addition to gasoline enable to simultaneously control gaseous and  
536 particulate matter emissions while increasing indicated efficiency with respect to standard  
537 gasoline combustion.

538

## 5.0 References

- 540 1. Wang, C., Xu, H., Daniel, R., Ghafourian, A., Herreros, J. M., Shuai, S. and Ma, X.  
541 (2013). Combustion characteristics and emissions of 2-methylfuran compared to 2,5-  
542 dimethylfuran, gasoline and ethanol in a DISI engine. *Fuel*. 103, 200-211, doi:  
543 <http://dx.doi.org/10.1016/j.fuel.2012.05.043>.
- 544 2. United States Environmental Protection Agency. (2014). Health. Available:  
545 <http://www.epa.gov/pm/health.html>. Last accessed 16th Jan 2015.
- 546 3. Anderson, J. O., Thundiyil, J. G., and Stolbach, A. (2012). Clearing the Air: A Review  
547 of the Effects of Particulate Matter Air Pollution on Human Health. *Journal of Medical*  
548 *Toxicology*. 8, 166-175, doi: [10.1007/s13181-011-0203-1](https://doi.org/10.1007/s13181-011-0203-1).
- 549 4. Gumbleton, J., Niepoth, G. and Currie, J. (1976). Effect of Energy and Emission  
550 Constraints on Compression Ratio. SAE Technical Paper [760826](https://doi.org/10.4271/760826), doi:[10.4271/760826](https://doi.org/10.4271/760826).
- 551 5. Harrington J. A. and Shishu R. C. (1973). A single-cylinder engine study of the effects  
552 of fuel type, fuel stoichiometry, and hydrogen-to-carbon ratio and CO, NO, and HC  
553 exhaust emissions. SAE [730476](https://doi.org/10.4271/730476), doi: [10.4271/730476](https://doi.org/10.4271/730476).
- 554 6. Muranaka, S., Takagi, Y. and Ishida, T. (1987). Factors Limiting the Improvement in  
555 Thermal Efficiency of S. I. Engine at Higher Compression Ratio. SAE Technical Paper  
556 [870548](https://doi.org/10.4271/870548), doi:[10.4271/870548](https://doi.org/10.4271/870548).
- 557 7. Kramer, F., Schwarz, C. and Witt, A. (2000). Effect of Compression Ratio on the  
558 Combustion of a Pressure Charged Gasoline Direct Injection Engine. SAE Technical  
559 Paper [2000-01-0250](https://doi.org/10.4271/2000-01-0250), doi:[10.4271/2000-01-0250](https://doi.org/10.4271/2000-01-0250).
- 560 8. Yin, T., Li, T., Chen, L. and Zheng, B. et al. (2014). Optimization of Compression Ratio  
561 of a Boosted PFI SI Engine with Cooled EGR. SAE Technical Paper [2014-01-2552](https://doi.org/10.4271/2014-01-2552),  
562 doi:[10.4271/2014-01-2552](https://doi.org/10.4271/2014-01-2552).
- 563 9. Okamoto, K., Ichikawa, T., Saitoh, K. and Oyama, K. et al. (2003). Study of Antiknock  
564 Performance Under Various Octane Numbers and Compression Ratios in a DISI  
565 Engine. SAE Technical Paper [2003-01-1804](https://doi.org/10.4271/2003-01-1804), doi:[10.4271/2003-01-1804](https://doi.org/10.4271/2003-01-1804).
- 566 10. Yamakawa, M., Youso, T., Fujikawa, T. and Nishimoto, T. et al. (2012). Combustion  
567 Technology Development for a High Compression Ratio SI Engine. *SAE Int. J. Fuels*  
568 *Lubr.* 5(1):98-105, doi:[10.4271/2011-01-1871](https://doi.org/10.4271/2011-01-1871).
- 569 11. Smith, P., Heywood, J. and Cheng, W. (2014). Effects of Compression Ratio on Spark-  
570 Ignited Engine Efficiency. SAE Technical Paper [2014-01-2599](https://doi.org/10.4271/2014-01-2599), doi:[10.4271/2014-01-2599](https://doi.org/10.4271/2014-01-2599).
- 571 12. Najafia, G., Ghobadiana, B., Tavakoli, T. (2009). Performance and exhaust emissions of  
572 a gasoline engine with ethanol blended gasoline fuels using artificial neural network.  
573 *Applied Energy*. 86, 630-639, doi:[10.1016/j.apenergy.2008.09.017](https://doi.org/10.1016/j.apenergy.2008.09.017).
- 574 13. Maji, S., Babu, M. and Gupta, N. (2001). A Single Cylinder Engine Study of Power,  
575 Fuel Consumption and Exhaust Emissions with Ethanol. SAE Technical Paper [2001-28-0029](https://doi.org/10.4271/2001-28-0029),  
576 doi:[10.4271/2001-28-0029](https://doi.org/10.4271/2001-28-0029).
- 577 14. Nakata, K., Utsumi, S., Ota, A. and Kawatake, K. et al. (2006). The Effect of Ethanol  
578 Fuel on a Spark Ignition Engine. SAE Technical Paper [2006-01-3380](https://doi.org/10.4271/2006-01-3380),  
579 doi:[10.4271/2006-01-3380](https://doi.org/10.4271/2006-01-3380).
- 580 15. Taniguchi, S., Yoshida, K. and Tsukasaki, Y. (2007). Feasibility Study of Ethanol  
581 Applications to A Direct Injection Gasoline Engine. SAE Technical Paper [2007-01-2037](https://doi.org/10.4271/2007-01-2037),  
582 doi:[10.4271/2007-01-2037](https://doi.org/10.4271/2007-01-2037).
- 583

- 584 16. Nakama, K., Kusaka, J. and Daisho, Y. (2009). Effect of Ethanol on Knock in Spark  
585 Ignition Gasoline Engines. SAE Int. J. Engines 1(1):1366-1380, doi:[10.4271/2008-32-  
586 0020](https://doi.org/10.4271/2008-32-0020).
- 587 17. Overington, M. and Thring, R. (1981). Gasoline Engine Combustion—Turbulence and  
588 the Combustion Chamber. SAE Technical Paper [810017](https://doi.org/10.4271/810017), doi:[10.4271/810017](https://doi.org/10.4271/810017).
- 589 18. Costagliola, M. A., De Simio, L., Iannaccone, S. and Prati, M. V. (2013). Combustion  
590 efficiency and engine out emissions of a S.I. engine fueled with alcohol/gasoline blends.  
591 Applied Energy. 111, 1162-1171, doi: <http://dx.doi.org/10.1016/j.apenergy.2012.09.042>.
- 592 19. Catapano, F., Di Iorio, S., Sementa, P. and Vaglieco, B. (2014). Characterization of  
593 Ethanol-Gasoline Blends Combustion processes and Particle Emissions in a GDI/PFI  
594 Small Engine. SAE Technical Paper [2014-01-1382](https://doi.org/10.4271/2014-01-1382), doi:[10.4271/2014-01-1382](https://doi.org/10.4271/2014-01-1382).
- 595 20. Stein, R., Anderson, J. and Wallington, T. (2013). An Overview of the Effects of  
596 Ethanol-Gasoline Blends on SI Engine Performance, Fuel Efficiency, and Emissions.  
597 SAE Int. J. Engines 6(1):470-487, doi:[10.4271/2013-01-1635](https://doi.org/10.4271/2013-01-1635).
- 598 21. Kar, K., Cheng, W. and Ishii, K. (2009). Effects of Ethanol Content on Gasohol PFI  
599 Engine Wide-Open-Throttle Operation. SAE Int. J. Fuels Lubr. 2(1):895-901,  
600 doi:[10.4271/2009-01-1907](https://doi.org/10.4271/2009-01-1907).
- 601 22. Deng, B., Yang, J. and Zhang, D. (2013). The challenges and strategies of butanol  
602 application in conventional engines: The sensitivity study of ignition and valve timing.  
603 Applied Energy. 108, 248-260, doi: <http://dx.doi.org/10.1016/j.apenergy.2013.03.018>.
- 604 23. Zhang, Z., Wang, T., Jia, M., Wei, Q., Meng, X. and Shu, G. (2014). Combustion and  
605 particle number emissions of a direct injection spark ignition engine operating on  
606 ethanol/gasoline and n-butanol/gasoline blends with exhaust gas recirculation. Fuel.  
607 130, 177-188, doi: <http://dx.doi.org/10.1016/j.fuel.2014.04.052>
- 608 24. Popuri, S. and Bata, R. (1993). A Performance Study of Iso-Butanol-, Methanol-, and  
609 Ethanol-Gasoline Blends Using a Single Cylinder Engine. SAE Technical Paper  
610 [932953](https://doi.org/10.4271/932953), doi:[10.4271/932953](https://doi.org/10.4271/932953).
- 611 25. Yang, J., Yang, X., Liu, J. and Han, Z. et al. (2009). Dyno Test Investigations of  
612 Gasoline Engine Fueled with Butanol-Gasoline Blends. SAE Technical Paper [2009-01-  
613 1891](https://doi.org/10.4271/2009-01-1891), doi:[10.4271/2009-01-1891](https://doi.org/10.4271/2009-01-1891).
- 614 26. Niass, T., Amer, A., Xu, W. and Vogel, S. et al. (2012). Butanol Blending - a Promising  
615 Approach to Enhance the Thermodynamic Potential of Gasoline - Part 1. SAE Int. J.  
616 Fuels Lubr. 5(1):265-273, doi:[10.4271/2011-01-1990](https://doi.org/10.4271/2011-01-1990).
- 617 27. Merola, S., Tornatore, C., Valentino, G. and Marchitto, L. et al. (2011). Optical  
618 Investigation of the Effect on the Combustion Process of Butanol-Gasoline Blend in a  
619 PFI SI Boosted Engine. SAE Technical Paper [2011-24-0057](https://doi.org/10.4271/2011-24-0057), doi:[10.4271/2011-24-  
0057](https://doi.org/10.4271/2011-24-<br/>620 0057).
- 621 28. Stansfield, P., Bisordi, A., OudeNijeweme, D. and Williams, J. et al. (2012). The  
622 Performance of a Modern Vehicle on a Variety of Alcohol-Gasoline Fuel Blends. SAE  
623 Int. J. Fuels Lubr. 5(2):813-822, doi:[10.4271/2012-01-1272](https://doi.org/10.4271/2012-01-1272).
- 624 29. Tornatore, C., Merola, S., Valentino, G. and Marchitto, L. (2013). In-Cylinder  
625 Spectroscopic Measurements of Combustion Process in a SI Engine Fuelled with  
626 Butanol-Gasoline Blend. SAE Technical Paper [2013-01-1318](https://doi.org/10.4271/2013-01-1318), doi:[10.4271/2013-01-  
1318](https://doi.org/10.4271/2013-01-<br/>627 1318).
- 628 30. Wigg, B., Coverdill, R., Lee, C. and Kyritsis, D. (2011). Emissions Characteristics of  
629 Neat Butanol Fuel Using a Port Fuel-Injected, Spark-Ignition Engine. SAE Technical  
630 Paper [2011-01-0902](https://doi.org/10.4271/2011-01-0902), doi:[10.4271/2011-01-0902](https://doi.org/10.4271/2011-01-0902).
- 631 31. Yang, J., Wang, Y. and Feng, R. (2011). The Performance Analysis of an Engine Fueled  
632 with Butanol-Gasoline Blend. SAE Technical Paper [2011-01-1191](https://doi.org/10.4271/2011-01-1191), doi:[10.4271/2011-  
01-1191](https://doi.org/10.4271/2011-<br/>633 01-1191).

- 634 32. Gu, X., Huang, Z., Cai, J., Gong, J., Wu, X. and Lee, C.-f. (2012). Emission  
635 characteristics of a spark-ignition engine fuelled with gasoline-n-butanol blends in  
636 combination with EGR. *Fuel*. 93, 611-617, doi:[10.1016/j.fuel.2011.11.040](https://doi.org/10.1016/j.fuel.2011.11.040).
- 637 33. Karavalakis, G., Short, D., Hajbabaie, M. and Vu, D. et al. (2013). Criteria Emissions,  
638 Particle Number Emissions, Size Distributions, and Black Carbon Measurements from  
639 PFI Gasoline Vehicles Fuelled with Different Ethanol and Butanol Blends. SAE  
640 Technical Paper [2013-01-1147](https://doi.org/10.4271/2013-01-1147), doi:[10.4271/2013-01-1147](https://doi.org/10.4271/2013-01-1147).
- 641 34. He, X., Ireland, J., Zigler, B. and Ratcliff, M. et al. (2010). The Impacts of Mid-level  
642 Biofuel Content in Gasoline on SIDI Engine-out and Tailpipe Particulate Matter  
643 Emissions. SAE Technical Paper [2010-01-2125](https://doi.org/10.4271/2010-01-2125), doi:[10.4271/2010-01-2125](https://doi.org/10.4271/2010-01-2125).
- 644 35. Thewes, M., Müther, M., Brassat, A. and Pischinger, S. et al. (2012). Analysis of the  
645 Effect of Bio-Fuels on the Combustion in a Downsized DI SI Engine. *SAE Int. J. Fuels  
646 Lubr.* 5(1):274-288, doi:[10.4271/2011-01-1991](https://doi.org/10.4271/2011-01-1991).
- 647 36. de Souza, M., Vianna, J., and Fraga, A. (1998). Study of an Engine Operating with  
648 Exhaust Gas Recirculation at Different Compression Ratios. SAE Technical Paper  
649 [982895](https://doi.org/10.4271/982895), doi:[10.4271/982895](https://doi.org/10.4271/982895).
- 650 37. Zhong S., Daniel R., Xu H. and Wyszynski M.L. (2010). Combustion and emissions of  
651 2,5-dimethylfuran in a direct-injection spark-ignition engine. *Energy & Fuels*. 24, 2891–  
652 2899 doi:[10.1021/ef901575a](https://doi.org/10.1021/ef901575a).
- 653 38. Daniel, R., Tian, G., Xu, H. and Shuai, S. (2012). Ignition timing sensitivities of  
654 oxygenated biofuels compared to gasoline in a direct-injection SI engine. *Fuel*. 99, 72-  
655 82, doi: <http://dx.doi.org/10.1016/j.fuel.2012.01.053>
- 656 39. Daniel, R., Tian, G., Xu, H., Wyszynski, M. L., Wu, X. and Huang, Z. (2011). Effect of  
657 spark timing and load on a DISI engine fuelled with 2,5-dimethylfuran. *Fuel*. 90, 449-  
658 458, doi:[10.1016/j.fuel.2010.10.008](https://doi.org/10.1016/j.fuel.2010.10.008)
- 659 40. Daniel, R., Wang, C., Xu, H. and Tian, G. (2012). Effects of Combustion Phasing,  
660 Injection Timing, Relative Air-Fuel Ratio and Variable Valve Timing on SI Engine  
661 Performance and Emissions using 2,5-Dimethylfuran. *SAE Int. J. Fuels Lubr.* 5(2):855-  
662 866, doi:[10.4271/2012-01-1285](https://doi.org/10.4271/2012-01-1285).
- 663 41. Mittal, V., Revier, B. and Heywood, J. (2007). Phenomena that Determine Knock Onset  
664 in Spark-Ignition Engines. SAE Technical Paper [2007-01-0007](https://doi.org/10.4271/2007-01-0007), doi:[10.4271/2007-01-0007](https://doi.org/10.4271/2007-01-0007).
- 666 42. Wu, X., Daniel, R., Guohong, T., Xu, H., Huang, Z. and Richardson, D. (2011). Dual-  
667 injection: The flexible, bi-fuel concept for spark-ignition engines fuelled with various  
668 gasoline and biofuel blends. *Applied Energy*. 88, 2305–2314,  
669 doi:[10.1016/j.apenergy.2011.01.025](https://doi.org/10.1016/j.apenergy.2011.01.025).
- 670 43. Heywood, J. B. (1988). *Internal Combustion Engine Fundamentals*. McGraw-Hill  
671 Higher Education.
- 672 44. He, B.-Q., Liu, M.-B. and Zhao, H. (2015). Comparison of combustion characteristics of  
673 n-butanol/ ethanol–gasoline blends in a HCCI engine. *Energy Conversion and  
674 Management*. 95, 101–109.
- 675 45. de O. Carvalho, L., de Melo, T. and de Azevedo Cruz Neto, R. (2012). Investigation on  
676 the Fuel and Engine Parameters that Affect the Half Mass Fraction Burned (CA50)  
677 Optimum Crank Angle. SAE Technical Paper [2012-36-0498](https://doi.org/10.4271/2012-36-0498), doi:[10.4271/2012-36-0498](https://doi.org/10.4271/2012-36-0498).
- 679 46. Kittelson, D. B. (1998). Engines and nanoparticles: a review. *Journal of Aerosol  
680 Science*. 29, 575–588, doi:[10.1016/S0021-8502\(97\)10037-4](https://doi.org/10.1016/S0021-8502(97)10037-4).
- 681 47. Anderson, J., Leone, T., Shelby, M. and Wallington, T. et al. (2012). Octane Numbers  
682 of Ethanol-Gasoline Blends: Measurements and Novel Estimation Method from Molar  
683 Composition. SAE Technical Paper [2012-01-1274](https://doi.org/10.4271/2012-01-1274), doi:[10.4271/2012-01-1274](https://doi.org/10.4271/2012-01-1274).



- 684 48. Storey, J., Barone, T., Norman, K., and Lewis, S. (2010). Ethanol Blend Effects On  
685 Direct Injection Spark-Ignition Gasoline Vehicle Particulate Matter Emissions. SAE Int.  
686 J. Fuels Lubr. 3(2):650-659, doi:[10.4271/2010-01-2129](https://doi.org/10.4271/2010-01-2129).
- 687 49. Di Iorio, S., Lazzaro, M., Sementa, P., Vaglieco, B. et al. (2011). Particle Size  
688 Distributions from a DI High Performance SI Engine Fuelled with Gasoline-Ethanol  
689 Blended Fuels. SAE Technical Paper [2011-24-0211](https://doi.org/10.4271/2011-24-0211), doi:[10.4271/2011-24-0211](https://doi.org/10.4271/2011-24-0211).
- 690 50. Vuk, C. and Vander Griend, S. (2013). Fuel Property Effects on Particulates In Spark  
691 Ignition Engines. SAE Technical Paper [2013-01-1124](https://doi.org/10.4271/2013-01-1124), doi:[10.4271/2013-01-1124](https://doi.org/10.4271/2013-01-1124).
- 692 51. Catapano, F., Di Iorio, S., Lazzaro, M. and Sementa, P. et al. (2013). Characterization of  
693 Ethanol Blends Combustion Processes and Soot Formation in a GDI Optical Engine,"  
694 SAE Technical Paper [2013-01-1316](https://doi.org/10.4271/2013-01-1316), doi:[10.4271/2013-01-1316](https://doi.org/10.4271/2013-01-1316).
- 695 52. Ojapah, M., Zhao, H. and Zhang, Y. (2014). Effects of Ethanol on Performance and  
696 Exhaust Emissions from a DI Spark Ignition Engine with Throttled and Unthrottled  
697 Operations. SAE Technical Paper [2014-01-1393](https://doi.org/10.4271/2014-01-1393), doi:[10.4271/2014-01-1393](https://doi.org/10.4271/2014-01-1393).
- 698 53. Bielaczyc, P., Szczotka, A. and Woodburn, J. (2014). The Impact of Fuel Ethanol  
699 Content on Particulate Emissions from Light-Duty Vehicles Featuring Spark Ignition  
700 Engines. SAE Int. J. Fuels Lubr. 7(1):224-235, doi:[10.4271/2014-01-1463](https://doi.org/10.4271/2014-01-1463).

701 **Abbreviations**

702	<b>Bu20</b>	20% vol 1-butanol in gasoline
703	<b>CAD</b>	Crank Angle Degrees
704	<b>COV</b>	Coefficient of Variation
705	<b>DC</b>	Direct Current
706	<b>DISI</b>	Direct-Injection Spark-Ignition
707	<b>E20</b>	20% vol ethanol in gasoline
708	<b>IMEP</b>	Indicated Mean Effective Pressure
709	<b>KLMBT</b>	Knock Limited Maximum Brake Torque
710	<b>MFB</b>	Mass Fraction Burned
711	<b>NA</b>	Naturally Aspirated
712	<b>PFI</b>	Port Fuel Injection
713	<b>PID</b>	Proportional Integral Differential
714	<b>PM</b>	Particulate Matter
715	<b>ULG</b>	Unleaded Gasoline
716	<b>VAF</b>	Volumetric Air Flow

717

718 **Acknowledgement**

719 This work was conducted in the Future Engines and Fuels Lab at the University of  
720 Birmingham and financially supported by the Engineering and Physical Sciences Research  
721 Council (EPSRC) through the Research Grant EP/F061692/1. The authors are grateful to the  
722 Jaguar Land Rover plc, Shell Global Solutions UK plc and Cambustion Ltd. for their great  
723 technical support throughout the research work. Also great thanks are extended to the  
724 technicians of the University of Birmingham, Mr. Carl Hingley and Mr. Peter Thornton for  
725 their assistance in the experiments.

726

727 **Contact Information**

728 Prof. Hongming Xu  
729 Head of Vehicle and Engine Technology Centre  
730 School of Mechanical Engineering  
731 University of Birmingham  
732 Birmingham  
733 B15 2TT, UK  
734

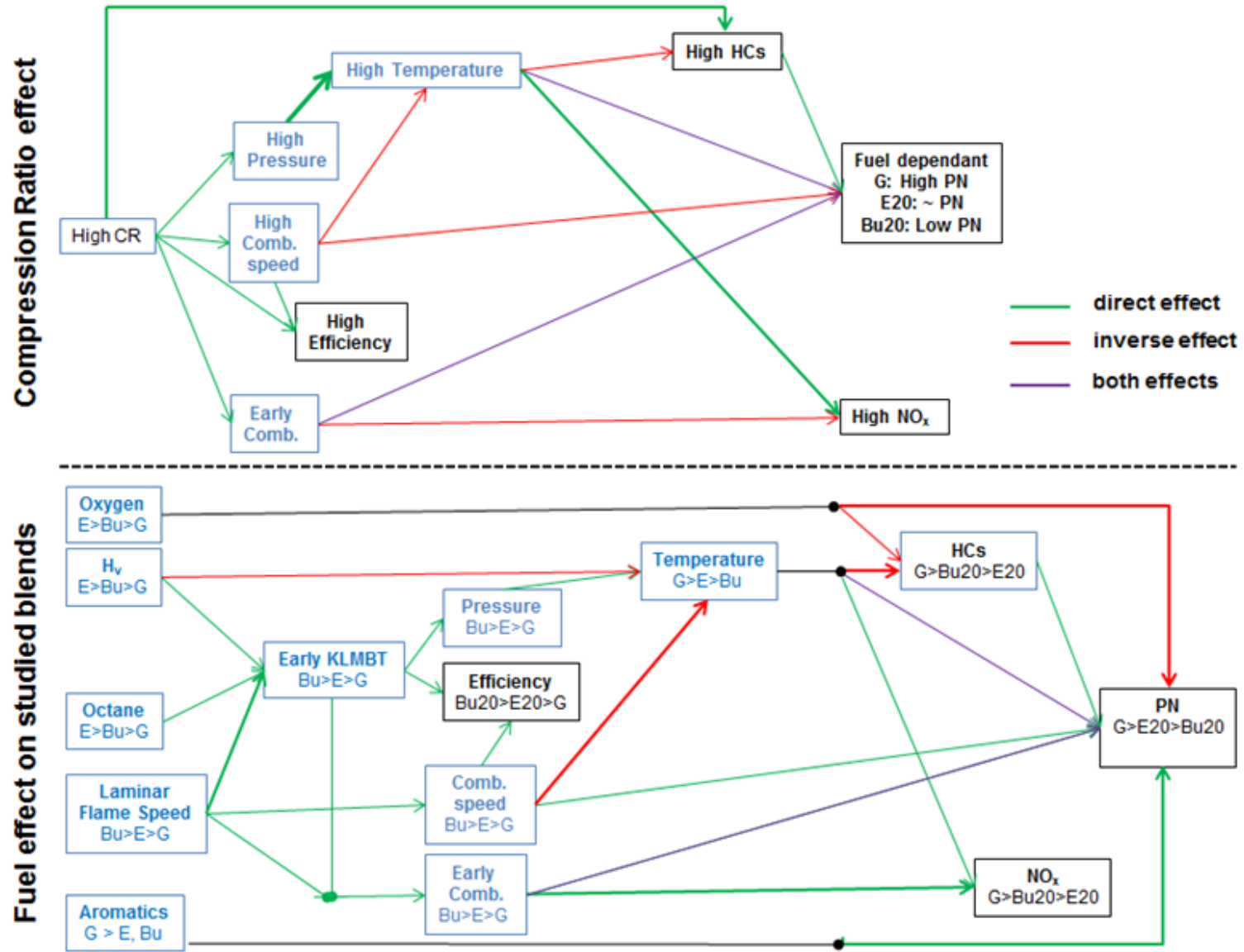


Fig. 8 Summary of compression ratio and fuel effects on combustion, fuel economy, gaseous and particulate matter emissions [Colour website, B&W print]